RESEARCH ARTICLE

From feeder dykes to scoria cones: the tectonically controlled plumbing system of the Rauðhólar volcanic chain, Northern Volcanic Zone, Iceland

Nadine Friese · Frithjof A. Bense · David C. Tanner · Lúðvík E. Gústafsson · Siegfried Siegesmund

Abstract The Rauðhólar volcanic chain, located in the Northern Volcanic Zone of Iceland, has been variably eroded such that, in the northern part, the original scoria cones are preserved, while the central and southern parts expose their shallow feeders. The chain thus offers insight into the inner workings of the near-surface feeder system of scoria cones. The volcanic chain was mapped in 3D using GPS. The en echelon-arranged volcanic chain can be divided into three parts: The southernmost part contains only plugs and necks with a thin pyroclastic cover as well as multi-tiered lava flows. The central part combines partially eroded scoria cones, (feeder) dyke intersections, and welded scoria interbedded within rootless and clastogenic lava flows; the welded scoria is composed of different kinds of lithics and bombs. The northern part preserves almost intact, overlapping scoria cones with voluminous lapilli-sized scoriaceous deposits. The overall dyke trend is orthogonal but shows radial patterns in individual cone complexes. Feeder dykes observed to depths of about 200 m below the volcanic chain are up to 8 m thick and flare in to conduits in the uppermost 20–50 m. The exposed shallow plumbing system shows that magma pathways through the volcanic edifice are very complex with incremental, repeated intrusions. We interpret the arcuate shape to be the result of a local change in the orientation of the stress field because the Rauðhólar volcanic chain is located within a major relay structure between volcanoes on the eastern Fremrinámur rift arm and a rift extension with grabens on the western periphery.

Keywords Scoria cone row · Hljóðaklettar · Rauðhólar · Northeast Iceland · Stress localization · Accommodation zone · Plumbing system

N. Friese (✉) · F. A. Bense · S. Siegesmund
Department of Structural Geology and Geodynamics, Geoscience Centre, University of Göttingen, Goldschmidtstrasse 3, 37077 Göttingen, Germany
e-mail: nfriese@gwdg.de

L. E. Gústafsson
Icelandic Association of Local Authorities, Borgartúni 30, 105 Reykjavík, Iceland

Present Address:
D. C. Tanner
Leibniz Institute for Applied Geophysics, Stilleweg 2, 30655 Hannover, Germany

Present Address:
N. Friese
Wintershall Norge AS, Kanalpiren, Labergel 28, 4020 Stavanger, Norway

Introduction

Rows of monogenetic volcanoes are the result of short-lived, small (<0.1 km^3) to medium (up to 1 km^3) volume eruptions of mafic to intermediate composition (Thordarson and Self 1993; Connor and Conway 2000). They can include scoria cones, tuff rings, and maars (Walker 1993). The traces of fissural eruptive segments are often marked by circular vent-type structures, most typically scoria and spatter cones, which are produced by combinations of effusive and explosive eruptions (e.g., Head and Wilson 1989; Thordarson and Larsen 2007). Scoria cones form as a consequence of Strombolian/Hawaiian to violent Strombolian activity (e.g., Houghton et al. 1999; Vespermann and Schmincke 2000; Martin and Nemeth 2006).

Fig. 1 a Generalized geological map of the fissure swarms in Northeastern Iceland, after Johannesson and Saemundsson (1998). *Encircled* central volcanoes are: *Th* Theistareykir, *Kr* Krafla, *Fr* Fremrinámur, and *As* Askja. Background is the DEM of Iceland provided by the National Land Survey of Iceland. **b** Geological map of the northern part of the Fremrinámur fissure swarm modified after Sigurdsson et al. (1975). The region where the studied Rauðhólar cone complex and Hljóðaklettar plugs are located is highlighted in *red*
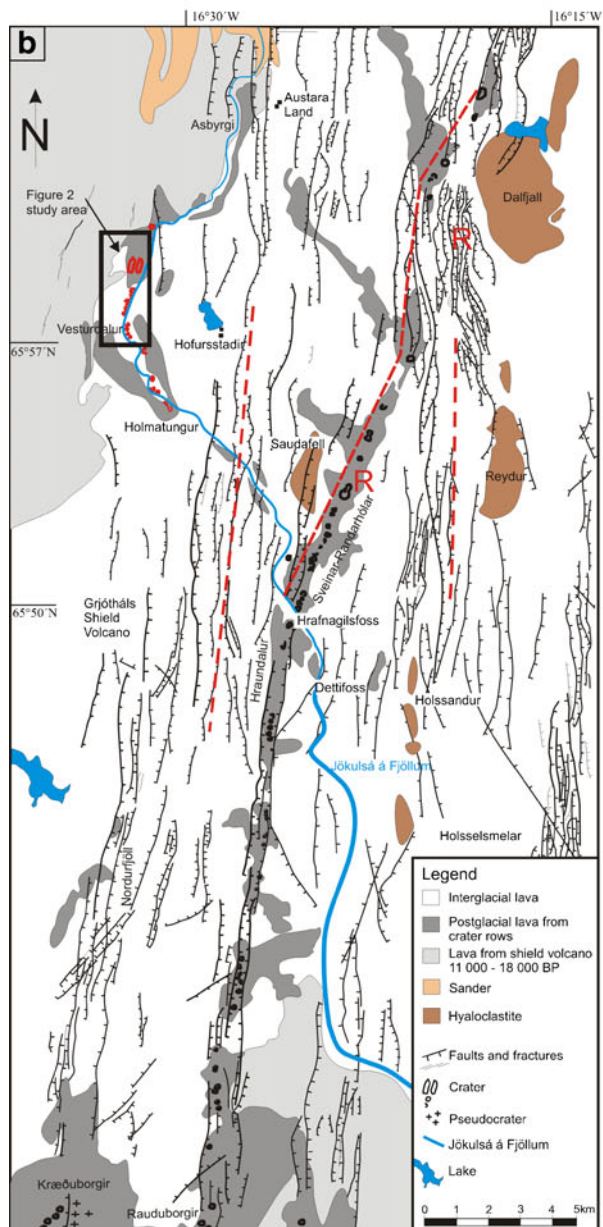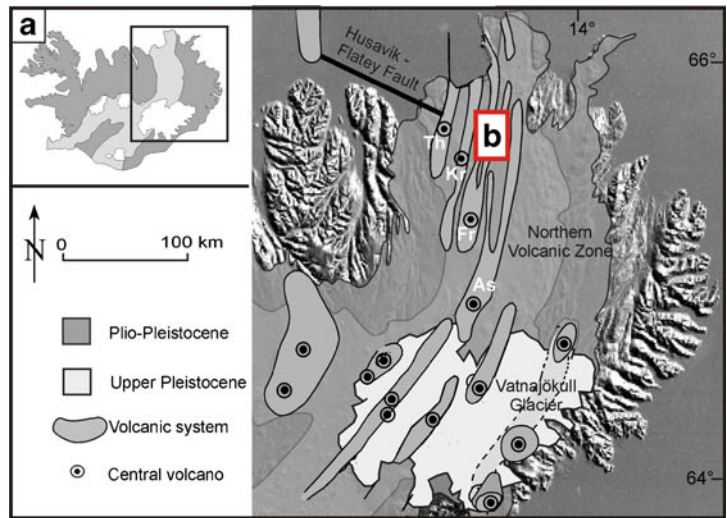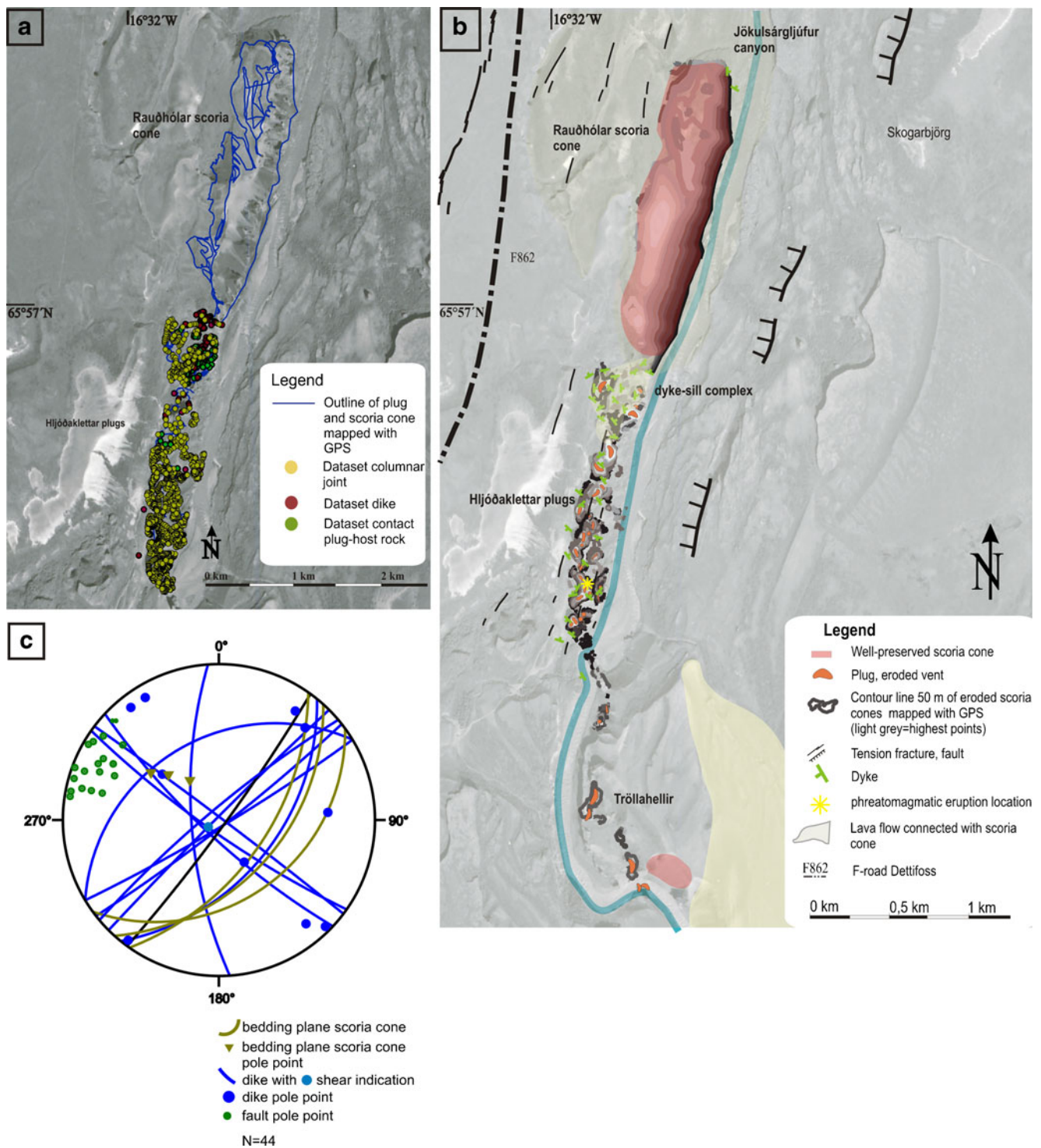
Fig. 2 a Dataset of measurements made in the field area. Two methods were used to collect point and line features (see text for further information). **b** Detailed geological map with faults, dykes, and cone geometries of the Rauðhólar cone chain. **c** Stereographic diagram of field data

Linear vent alignments and dykes are stress indicators and have been used as data sources in the world stress map (Nakamura 1977; Heidbach et al. 2008) and in paleostress analysis (Vespermann and Schmincke 2000; Bosworth et al. 2003; Paulsen and Wilson 2010). The distribution of monogenetic vents provides a good indication of the pathways that were opened by feeder dykes during their ascent through the crust (e.g., Nemeth and White 2003; Valentine
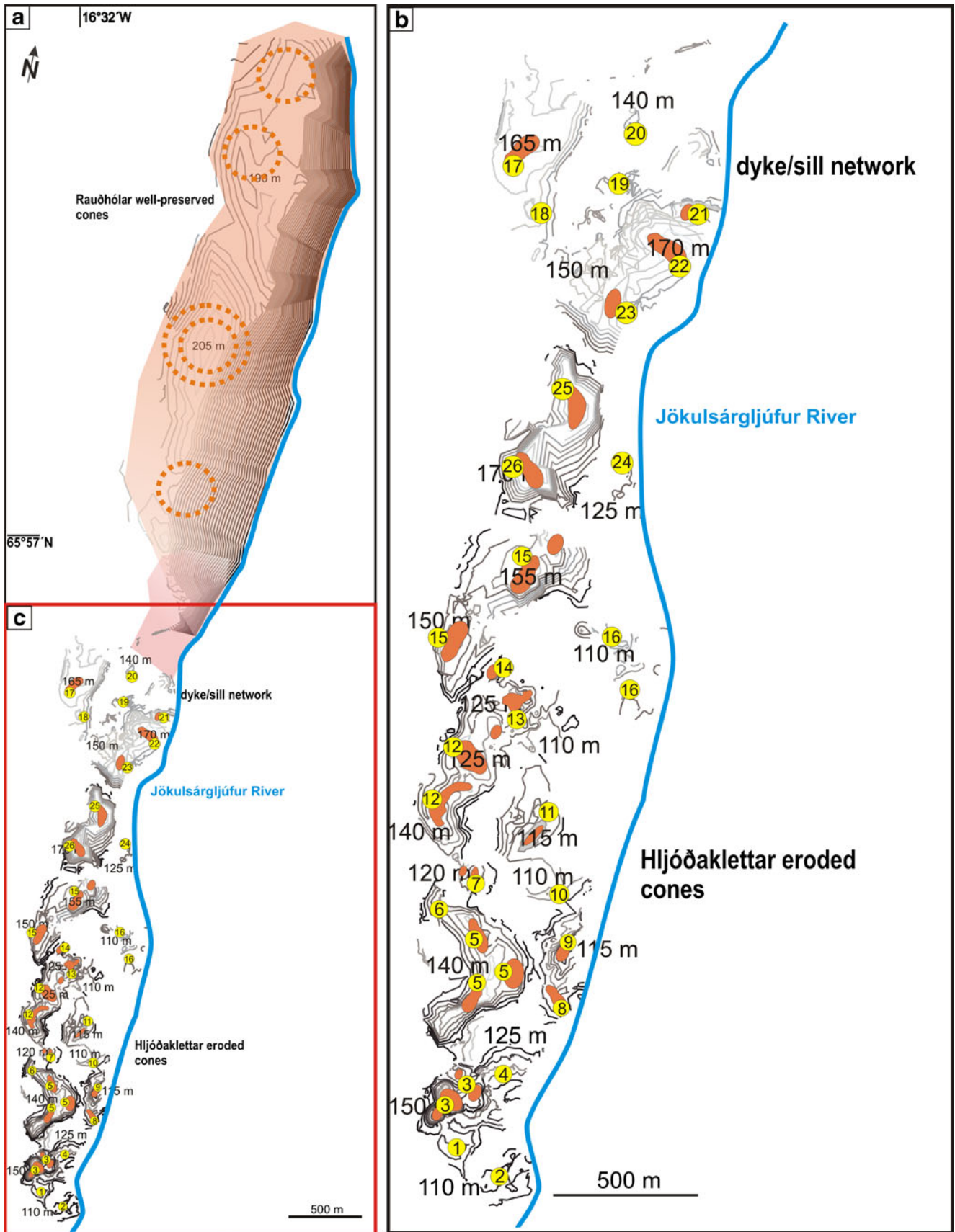
◀ **Fig. 3** **a** Contour map of the cone row topography of the plugs and inferred eruptive vents (*dotted orange circles*) indicated by contours of different colors (*dark* low altitude to *light* higher altitude above sea level; contour lines at 10-m intervals). The locations of plug data (Table 1) are shown as *yellow circles*. The row is formed by 26 plug complexes and 35 dykes measured in the field. The altitude of the base of the volcanic chain has an average elevation of 100 m, while the bottom of the river canyon has an average elevation of 50 m. See also the Supplementary data of the volcanic chain available online. **b** Close-up view of the central and southern part of the volcanic chain

and Keating 2007; Mazzarini 2007; Keating et al. 2008; Rooney et al. 2011).

Only a few monogenetic eruptions have been witnessed that give insight into eruption dynamics. Key examples are the 1943–1952 Paricutin eruption, Mexico (Luhr and Simkin 1993; Pioli et al. 2008); the 1973 Heimaey eruption, Iceland (Self et al. 1974); and the 1975–1976 Tolbachik fissure eruption, Kamchatka (Fedotov and Markhinin 1983). Hence, valuable information on the eruption mechanisms can be gathered from studies of eruptive deposits (e.g., Valentine et al. 2005; Valentine and Krogh 2006; Valentine and Keating 2007), geochemical studies (e.g., Brenna et al. 2010; Erlund et al. 2010), and by studying eroded cones (e.g., Nemeth and White 2003; Valentine and Krogh 2006; Keating et al. 2008). Well-monitored eruption examples, such as the Krafla fires 1975–1984 in the Krafla fissure swarm, Iceland (e.g., Tryggvason 1980, 1994; Brandsdottir et al. 1997), also yield information about sub-surface processes such as dyke propagation (Björnsson et al. 1977; Buck et al. 2006).

Indications of the interaction of magma and the surface can be observed at cone rows that were eroded differentially, where the vent systems are exposed as complex multiple dyke–sill networks (e.g., Johnson et al. 2008; Keating et al. 2008). The Rauðhólar volcanic chain is an early Holocene, monogenetic eruptive fissure situated in the Northern Icelandic Fremrinámur volcanic system (Fig. 1). Due to the deeper erosion of the southern part of the volcanic chain by the Jökulsá á Fjöllum River, the interiors of the Rauðhólar cones are exposed up to a depth of 200 m and allow the direct observation of the shallow plumbing system, while cones on the northern part of the chain are nearly uneroded. This site is a natural laboratory that offers the opportunity to study a 3D, near-surface cross-section through the inner workings of a scoria cone row in detail.

The aim of this paper is to document the exposed early Holocene eruptive fissure in three spatial dimensions, to re-construct the eruptive dynamics, and to describe the controls on emplacement and propagation of magma beneath a small eruptive complex. The study employs detailed 3D mapping of the volcanic construction (see the Supplementary data), which was necessary because of the inaccurate digital elevation model (DEM) of the area. The 3D shapes of the plugs are used to determine the magma flow, feeder dyke segmentation, and localization of the eruptive centers.

Regional setting

Plate spreading in Iceland is confined to rift zones, such as the Northern Volcanic Zone, which represent emergent parts of the Mid-Atlantic Ridge (see inset in Fig. 1a). Individual volcanic systems form en echelon arrays, where each segment is connected to a central volcano as the main source of volcanic production (Fig. 1a). The average spreading rate in the northern part of Iceland is 1.8 cm a^{-1} in a N106°E direction, based on the NUVEL-1A model (DeMets et al. 1994) and current GPS measurements (Arnadottir et al. 2009).

Rift-related structures and eruptive fissures are common in the Northern Volcanic Zone, but early postglacial and interglacial lava shield volcanoes were responsible for the major lava production (MacLennan et al. 2002; Fig. 1b). The focus of this study is the early Holocene Rauðhólar crater row, which is located at the western margin of the 160-km-long, up to 17-km-wide, NNE trending Fremrinámur volcanic system (Fig. 1). The central volcano of the system is located at its southernmost end and is constructed on the basaltic Ketildyngja shield volcano, which is in turn overlain by two lava shields (Johannesson and Saemundsson 1998; Hjartardottir 2008). The last eruption of the Ketildyngja shield volcano occurred 4,000 years ago (Thorarinsson 1951). The Fremrinámur volcanic system branches north-wards, which makes the assignment of individual volcanic chains (mainly discontinuous spatter and scoria cones) and fissures to particular central volcanoes challenging because parts of the westerly branch of the Askja volcanic system are very close (Fig. 1a). For example, Tentler and Mazzoli (2005) attributed the individual crater rows, known as Kræðuborgir, Sveinar–Randarhólar, and Rauðhólar, to the Fremrinámur system (Fig. 1b), whereas the same volcanic chains were assigned to the Askja fissure swarm by Johannesson and Saemundsson (1998) and Hjartardottir (2008).

The Rauðhólar volcanic chain and its southern eroded part (called Hljóðaklettar; Figs. 1b, 2b, and 3) are regarded here as the westernmost branch of the Fremrinámur fissure swarm (Fig. 1b) and crop out along the narrow river canyon of Jökulsá á Fjöllum as aligned, small-volume scoria cones, plugs, and volcanic necks; a few vents are located inside the canyon. The approximately 6-km-long vent system is aligned NNE, while at its southern end, it bends slightly NNW, giving it an arcuate shape (Figs. 1b and 2b). As the cones underlie the Hekla tephra H5 deposits (dated to 6,000 years BP; Thorarinsson 1971; Kirkbride et al. 2006), the Rauðhólar eruption is estimated to be of early Holocene age, around

Table 1 Data set of all measured and mapped volcanic plug complexes in the Rauðhólar volcanic chain

| Plug GPS coordinates	Plane view shape	Diameter	Cross-section shape	Paleo-surface depth to convergence feeder dike	Description and remarks
1. N 606437; E 612144	Irregular, round–elongated	5 m	Round–elongated		Bifurcating dyke–sill network
2. N 606391; E 612195	Irregular, elongated	5 m	Elongated		Dense dyke–sill network, vesicles
3. N 606496; E 612222	Circular to elongated with long axis towards NNE, multiple plugs, connected	15–50 m	Cylindrical to equant shape	20 m at the southern part	Multiple dyke intrusion phases welded spatter at top, vesicles
			Flaring to conduits, oval		Connected by sills, columnar joints
					Olivine, plagioclase crystals; dike splays at northern end; hyaline margin
					Basalt xenolith
4. N 606515; E 612208	Elongated, long axis NNE	50–120 m	Elongated, oval	Flaring upper 15 m	Multiple, bifurcating dykes, welded
					Hyaline margin, redial columnar joints
5. N 606574; E 612257	Elongated, planar, distinctive horseshoe shape	100–130 m	Oval, irregular	15–20 m?	Multiple plugs; welded scoria margin
					0.2 m chilled margin to host rock
					Bombs, xenoliths, vesicles
6. N 606667; E 612127	Elongated, bend	20 m	Irregular–cylindrical		Welded scoria, radial columnar joints
7. N 606624; E 612282	Linear–round	25 m	Linear, cone-shaped	10 m	Welded, scoria, radial columnar joints
					Small plugs connected by 2-m-high dyke
8. N 606626; E 612134	Round–elongated	4 m	Slightly cylindrical		Chilled margin, connected by irregular 0.5- to 2-m-thick multiple dyke, scoria
9. N 606667; E 612127	Roundish irregular	10 m	Irregular	5 m?	Margin, radial columnar jointing
10. N 606702; E 612256	Round	10 m	Round		Columnar jointing, highly eroded
11. N 606731; E 612208	Roundish, elongated	15 m	Roundish		Columnar jointing, multiple plugs?
					Highly eroded
12. N 606928; E 612204	Irregular, elongated	50 m	Elongated, planar	10–15 m?	Welder spatter, dyke splays in host rock, bifurcating multiple intrusions
13. N 606892; E 612360	Irregular	35 m	Cone-shaped to roundish	25 m	Thick constant conduits, multiple wavy, bifurcating dykes
14. N 606928; E 612204	Elongated	20 m	Planar, linear		Thick, parallel (stacked?) dyke
15. N 606928; E 612196	Horseshoe shape	120–150 m	Planar, rectangular	Possible upper 3 m	Multiple bifurcating dyke, chilled margins, flat top
16. N 606872; E 612291	Round	2–5 m	Round		Low altitude, columnar joints, rich in vesicles, "field" of small plugs
17. N 607517; E 612283	Roundish rectangle	150 m	Planar, rectangle		Flat top, linear columnar joints
					Constant width
18. N 607352; E 612242	Linear, elongated	10 m	Elongated		Flat, strongly eroded

Table 1 (continued)

Plug GPS coordinates	Plane view shape	Diameter	Cross-section shape	Paleo-surface depth to convergence feeder dike	Description and remarks
19. N 607415; E 612310	Linear, elongated	5–10 m	Planar–elongated		Bending sill "roof" on top of welded scoria, strongly eroded, plug field
20. N 607470; E 612332	Linear, elongated	2 m	Planar		Dyke connected to plug, welded front
21. N 607467; E 612418	Round	10 m	Cone-shaped, oval		Strongly eroded, inclined 5 m thick. Multiple dyke as "roof," fault?
22. N 607403; E 612428	Elongated	110 m	Cone-shaped, linear Flaring to conduits	15 m	Welded scoria walls, bifurcating, multiple dykes and sills
23. N 607305; E 612364	Linear	20 m	Linear, planar	5 m	Merging dykes to linear conduit
24. N 607138; E 612329	Irregular	3 m	Planar		Vesicles
25. N 607236; E 612302	Elongated	150 m	Cone-shaped, equant	5–10 m	Dyke flaring, constant width, massive basalt plug, welded scoria front
26. N 607068; E 612184	Elongated	75 m	Cone-shaped, equant	5–10 m	Welded scoria and dyke alternating. Dyke flaring, constant width, massive

9,000 years BP (Waitt 2002 and references therein; Tentler and Mazzoli 2005). The deposits of the Rauðhólar volcanic chain overlie an intra-canyon lava flow that covers an area of 2 km² , which is located just west of the valley of Vesturdalur (Fig. 1b). The cross-cutting relationships of the lava flow show that the paleo-Jökulsá River had produced a canyon, nearly to its present depth, before the onset of the Rauðhólar eruption (Alho et al. 2005).

Stacked lava flows that surround the vent row can be followed for large distances (Thorarinsson 1959; Höskuldsson and Thordarson 2002; Kirkbride et al. 2006). These lava flows were sourced from shield volcano eruptions (e.g., Grjótháls eruption and partial lava from the Randaholar–Rauðborgir fissure; Fig. 1b; Slater et al. 1998), which occurred more than 11,000 years ago, since they underlie the Rauðhólar scoria cones and were only exposed by erosion along the river canyon. Isolated hyaloclastite mountains that formed during the last glacial phase are the subglacial analogue of present-day subaerial fissure eruptions (Saemundsson 1979) and flank the Fremrinámur system on its northern end (Fig. 1b). The lava flows east of the Rauðhólar/Hljóðaklettar area formed during a >10,000-year-old eruption from a shield volcano in the nearby Þeistareykir fissure swarm (Information Centre Jökulsárgljúfur; Fig. 1a), which consequently dammed the lower valley and diverted the paleo-Jökulsá River. The slightly younger (6,000–8,000 years BP; Thorarinsson 1959; Sigurdsson et al. 1975; Tentler and Mazzoli 2005; Fig. 1b), NNE trending, around 70-km-long Randaholar–Rauðborgir fissure to the southeast of the Rauðhólar volcanic chain is the most prominent volcanic fissure in the Fremrinámur volcanic system. This linear scoria cone chain coincides with graben-bounding normal faults that are connected to the Fremrinamur Central Volcano (Fig. 1a), located further to the south. Part of the lava of the Randaholar–Rauðborgir volcanic chain flowed northwards and overlaid the lava of the Rauðhólar eruption. The magma of both fissural eruptions is primitive olivine tholeiitic (Information Centre Jökulsárgljúfur).

We infer that the <120-m-deep Jökulsá á Fjöllum canyon was excavated by numerous gigantic glacial outburst floods (16 outbursts were documented by stratigraphic methods near Vesturdalur; Waitt 2002) that originated from the Vatnajökull Glacier to the south (Fig. 1a). The largest outbursts occurred between 7,100 and 2,000 years BP and probably just after the deglaciation around 9,000–8,000 years BP (Waitt 2002; Alho et al. 2005 and references therein; Kirkbride et al. 2006). We infer that one or more of the outbursts eroded parts of the Rauðhólar volcanic chain, leaving the more resistant plugs and dykes exposed in the central and southern parts of the Rauðhólar vent row, which are known now as Hljóðaklettar (Figs. 2b and 3). It has been argued that most of the Jökulsá canyon already existed in its present form before the Holocene
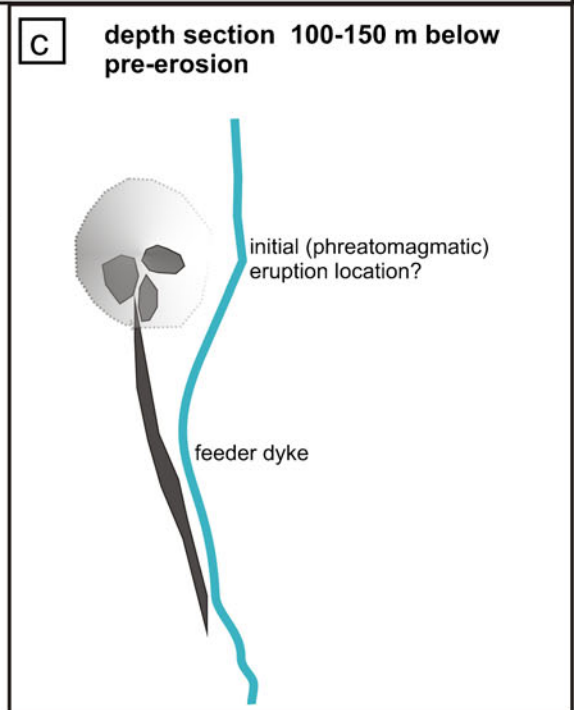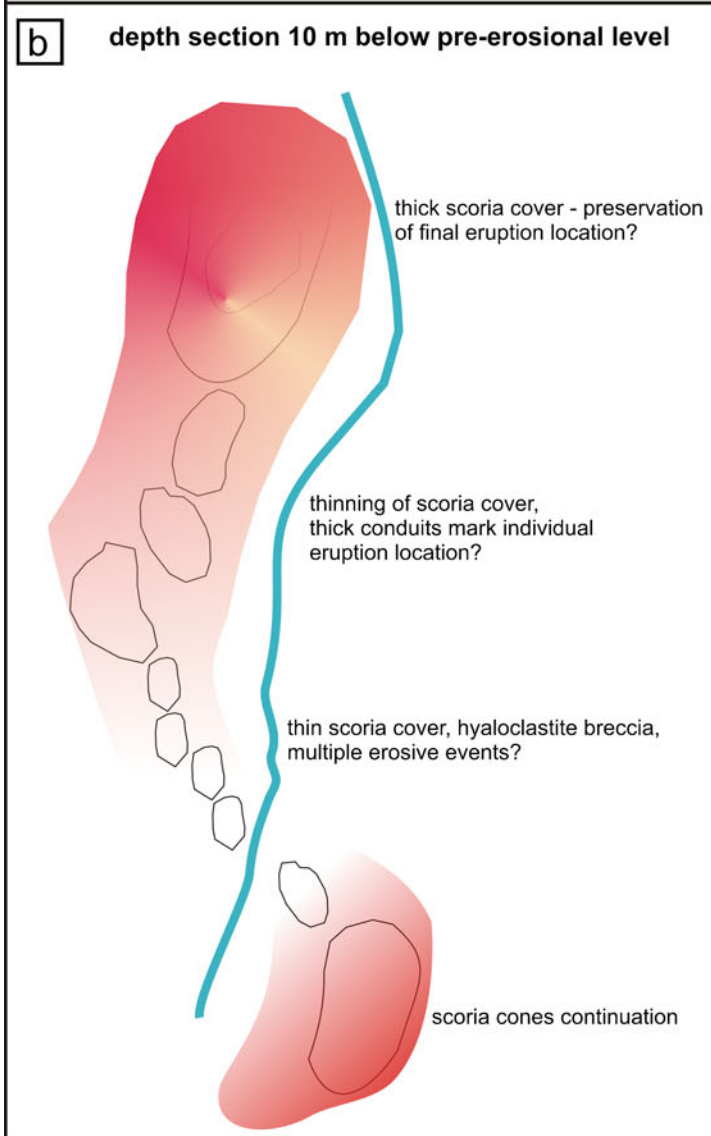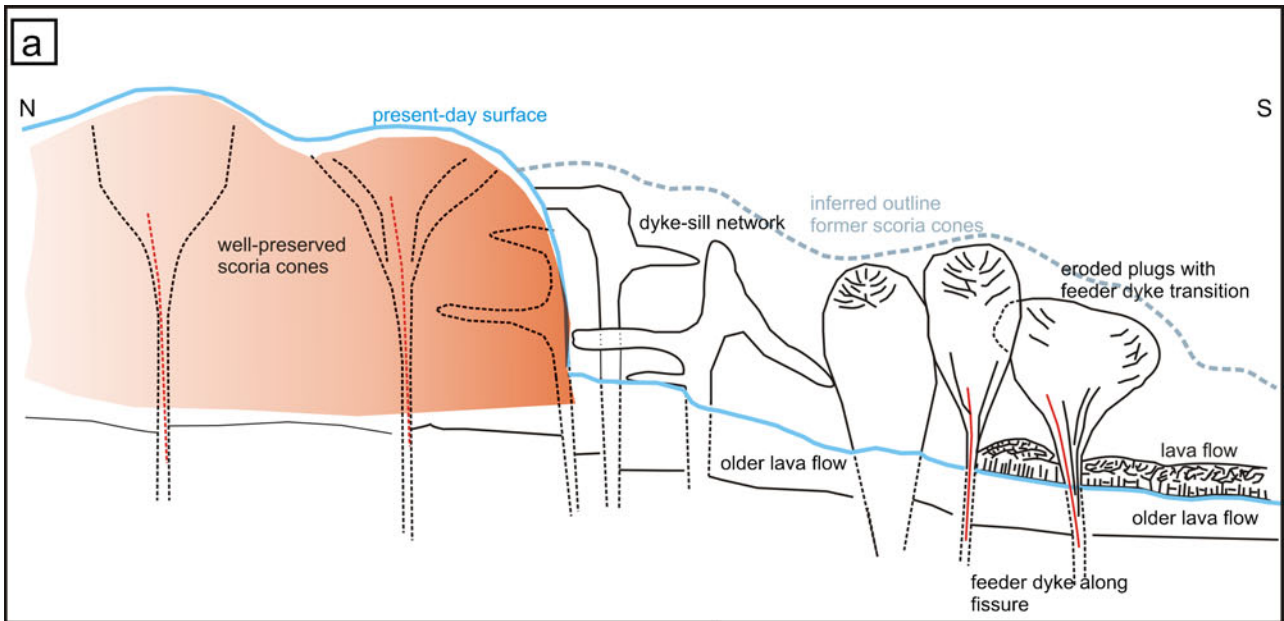
◀ **Fig. 4** **a** Schematic north–south cross-section through the Rauðhólar volcanic chain to highlight the three major sections. **b** Conceptual depth section at around 10 m below the pre-eruptive surface, illustrating different scoria thicknesses and the location of tops of magma conduits. **c** Depth section of the volcanic chain 100–150 m below the pre-erosional surface showing the initial phreatomagmatic eruption in connection with feeder dyke intrusion

floods, as the valley cuts into a preglacial to late glacial basalt (Kirkbride et al. 2006). The southern part of the Jökulsá exposes an almost continuously stacked lava flow interbedded with hard tillite/palagonite, breccia, and several thin tephra layers that have been used for geochronological dating (Hekla tephra H3–H5, which corresponds to ages ranging from 2,900 to 6,000 years BP; Thorarinsson 1959; Kirkbride et al. 2006). A detailed canyon morphology, stratigraphy, and glacial outburst history is given by Waitt (2002) and Alho et al. (2005).

Field data acquisition and 3D model of the Rauðhólar volcanic chain

The well-preserved Rauðhólar cones at the northern end of the volcanic chain and the eroded vents that correspond to the Hljóðaklettar plugs were mapped with a mobile Trimble Pathfinder® ProXH™ GPS system, including a 12-channel, dual-frequency GPS receiver, a Zephyr antenna, and a Ranger™ field computer, with an accuracy of 0.4 m in the horizontal direction and 0.7 m in the vertical direction, after post processing. The accuracy of mapping for the individual plugs in the field depended mainly on satellite availability and the geometry of the plugs. Data recorded with the GPS equipment include the outline of each plug, orientation data on individual dykes (including strike, dip, and thickness), attitude data of volcaniclastic bedding planes, and faults in the vicinity of the volcanic chain (Fig. 2a, b). A total of 20 minor and major faults, 26 plug complexes, and 35 individual dykes were mapped in the accessible part of the Rauðhólar volcanic chain (Figs. 2 and 3; for plug data, see Table 1).

Structural data were obtained by two different methods: point and line feature measurements. With point measurements, a structural feature was defined by a number of points, each one with known coordinates and spatial orientation (strike and dip); dykes and their contacts with the host rock were measured in this way. The line feature method was used to map the complete 3D outline of a plug by continuously walking around and over the feature. The heights of unscalable plugs were measured with a Silva leveling clinometer.

Smaller inaccessible areas, such as overhanging parts of the plugs, were reconstructed with the help of aerial photographs in ArcGIS 9.1; this information was later added manually to the 3D model of the volcanic chain. Aerial photographs at the scale of 1:30,000, a DEM of the area (cell size of 25 m) provided by the National Land Survey of Iceland, and several digital maps (available on the National Land Survey Iceland webpage http://www.lmi.is) were used as topographic base maps to plot field data and the individual plug outlines that were determined by GPS measurements (Figs. 2 and 3). The digital maps and the DEM were also used to reconstruct the mapped field point-sets and surface structures onto the 3D shape of the current volcanic chain morphology using the softwares GoCad 2.0.8, 3D Move 5.0, and Move 2008.1 (Supplementary data).

Part of the southernmost area of the cone row, east of the Jökulsá á Fjöllum canyon, across the river, could not be mapped in the field due to limited accessibility and, therefore, had to be left out of the modeled 3D reconstruction. However, its general vent alignment (strike direction of the eruptive fissure) and morphology, as seen on aerial photographs, was included in the overall interpretation of the entire Rauðhólar volcanic chain.

Shape and deposits of the volcanic chain

Map view and vertical cross-section of the volcanic chain

A cross-section through the volcanic chain shows the main magmatic sections and the plumbing system of the cone row: (1) the northern well-preserved scoria cones, (2) the adjacent dyke–sill network, and (3) eroded plugs, partly with transitions to its feeder systems in the central and southern part, and multi-tiered lava flows at the southernmost chain section (Fig. 4a). Planes of different levels through the volcanic chain illustrate its pre-erosional shape (Fig. 4b, c).

The reconstructed 3D shape of the system shows that the eruptive vents are offset in a left lateral manner. The vents are closely spaced, with intervals of 50–300 m (Fig. 3). The well-preserved northern Rauðhólar cones are spaced 200 m apart in N–S direction and up to 800 m in E–W direction (Fig. 3). The height of the plugs varies between 10 and 190 m, and the well-preserved cones reach up to 205 m (Fig. 3). Overall, the vent height increases gradually to the north. The outline of the N–S trending (around 2,000 m long), well-preserved Rauðhólar scoria cone suggests that it consists of at least two partially buried and overlapping cones (coalescing cones; Fig. 3).

In map view, the necks and cones in the southern and central parts of the chain are up to 150 m in diameter, most of them are elongated in an overall NNE–SSW direction, while others are horseshoe-shaped and irregularly shaped (Figs. 2b and 3; Table 1; see the Supplementary data). In vertical exposures, they are consistently equant, planar-

Table 2 Different lithofacies types and interpretation of the main pyroclastic deposits in the Rauðhólar volcanic chain

Lithofacies type	Location of occurrence	Description	Interpretation	Figures
Nonwelded to weakly welded red and dark brown scoriaceous lapilli	Northern end of Rauðhólar scoria cone complex, well-preserved cones	Medium-grained to coarse-grained, well-sorted, well-bedded, oxidized, partly flattened, monotonous Fall deposit thickness decreases rapidly away from vent, absent 500 m to the east, western part post-depositional eroded	Strombolian eruption style	6a–e
		Diffuse internal stratification, clast-supported, parallel, towards vent center-dipping beds (20–50°)	Emplaced on the inner slopes of vent?	6a–c
	Canyon wall facing the river, northern end of scoria cones	Rootless lava flows embedded in loose scoria		6b–c, f
Interbedded volcanic bombs	Northern part of the cone row	Cored bombs, fusiform, rounded bombs mantled by scoria lapilli and agglutinated spatter	Strombolian eruption type	8a, b
Twisted, fluidally shaped, welded red and black scoria and breccia	Steep inner wall, adjacent to well-preserved scoria cones, and central cone row part	Welded vent breccia diameter up to 20 cm; clasts are spindle, fluidally shaped and ribbon-shaped; clastogenic lava flow	Transitional Strombolian to Hawaiian eruption style	7a–c
Interbedded volcanic bombs and blocks	Angular blocks and rounded bombs in basal part of plug (local occurrence at transition between southern and central part)	Cored and rounded ballistic bombs mantled by scoria lapilli and agglutinated spatter Up to 30 cm in diameter, angular to well-rounded angular blocks of tholeiite with plagioclase and olivine phenocrysts	Gravel from river, and blocks from underlying lava flow Phreatomagmatic eruption	8c, d
Granular flow deposits	Northernmost end of scoria cone complex, small outcrop	Plainly stratified beds, thickness 0.1–0.5 m Pinch and swell structures, low-angle stratification, small-scale ripples Uppermost layer contains well-rounded, well-sorted black–red lapilli up to 1 cm diameter	Granular flows on cone slopes at end of Strombolian eruption	9a–c

shaped to funnel-shaped and represent the convergence and intersection points of several bifurcating sills and dykes (Fig. 5). This widening of some of the conduits is documented to begin at 5–20 m below the inferred paleo-surface (Table 1). Other plugs show a constant conduit width of up to 110 m in diameter from bottom to top. Individual plugs (complexes) are connected by linear dykes and sills (see below; Figs. 4a and 5a, b, e). The elongated shape of the plugs in map view is a consequence of this complex coalescence of dykes and sills.

Pyroclastic deposits

Stratigraphic profiles were not used to reconstruct the eruption sequence, as large parts of the system are eroded, and the pyroclastic deposits are largely restricted to the vent row itself. Scoria deposits associated with the Rauðhólar eruptions are absent more than 500 m east or west of the vent row. Pyroclastic deposits can be grouped by their grain size, clast shape, and degree of welding into three types: (1)

nonwelded to weakly welded red and dark brown scoriaceous lapilli, interbedded with fluidal and cored bombs, at the northern end of the volcanic chain, (2) deposits that are interpreted to result from granular flows on cone slopes are also found at the northern Rauðhólar part, and (3) twisted, fluidally shaped, welded spatter and scoria with localized occurrence of clastogenic lava flows, volcanic bombs, and angular blocks in the central part of the volcanic chain (Table 2; Figs. 6, 7, 8, and 9). The plugs in the southernmost part are covered with a thin layer of volcaniclastic breccias and scoria remnants (Fig. 12); these are not regarded as a separate deposit.

The central dyke–sill complex and eroded plugs in the Hljóðaklettar area

The area between the Rauðhólar well-preserved scoria cones and the eroded Hljóðaklettar plugs (Figs. 2b and 3) is characterized by a subvertical and horizontal intersecting, linear, cross-cutting dyke–sill complex (Figs. 4a and 5),
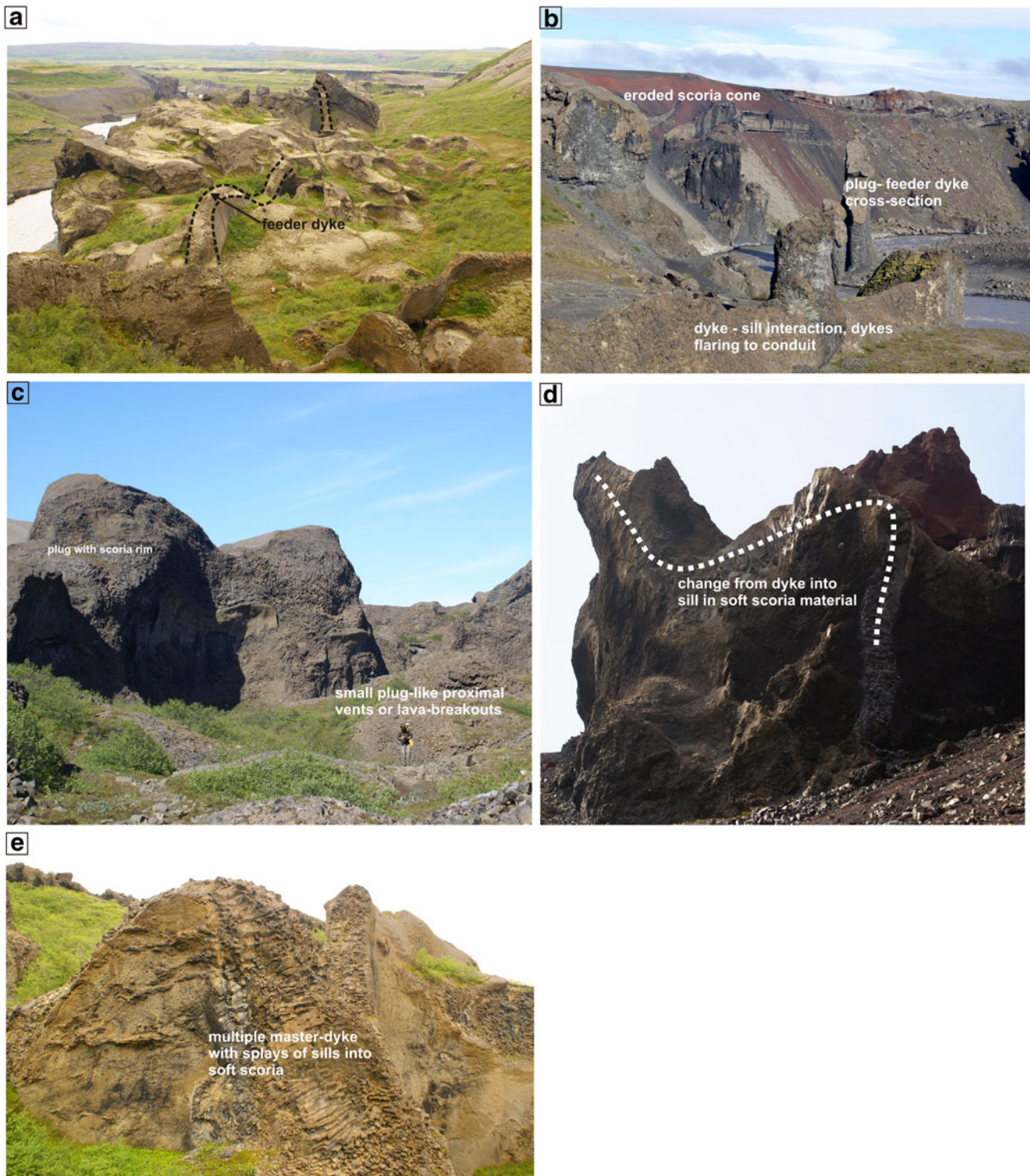
Fig. 5 Plug and dyke–sill network in the Hljóðaklettar area. **a** View towards S to the dyke–sill network located between the well-preserved scoria cones and the centrally located plugs. The dyke walls are approximately 15–20 m high. A feeder dyke can be followed through the entire outcrop (*dashed line*). **b** Plugs exposed at the southern edge of Hljóðaklettar located in the river canyon. **c** Plugs, up to 40 m high, with a thin clastic cover. **d** Attitude change in an intrusion formed during magma ascent towards the surface. **e** Sill-like protrusions in a small plug with multiple dyke injections

which represents the shallow plumbing system beneath the cones. Gradually southwards, the occurrence of discrete, linear stand-alone (feeder) dykes decreases and grades into multiple intrusions that feed the plugs.

Fig. 6 Pyroclastic deposits of the Rauðhólar volcanic chain. **a** Panoramic view towards N. Pyroclastic beds are visible on the outer hinge. *Arrows* point to persons used as scale. Jökulsárgljúfur canyon is in the background. **b** View of the eroded part of scoria cone. One-meter-thick rootless lava flows (*arrow*) are interlayered with pyroclastic fall deposits. View to the northeast. **c** Inclined intrusion embedded in pyroclastic fall deposits. Grain size ranges from lapilli to small bombs. View to the northeast. **d** Diffusely layered scoria cone deposit containing scoriaceous lapilli, small fluidally elongated bombs. Compass for scale. View to the NNW. **e** Close-up view of **d**. **f** NNW view of the inner part of the Rauðhólar cone complex, which was exposed by fluvial erosion during glacial outbursts. Lava plugs with brownish hyaloclastite cover show entablature structure

The overall dyke trend is orthogonal NE–SW and NW–SE (Fig. 2c), but locally, a radial pattern within the cone complexes can be observed (Fig. 2b), where the stress field was strongly modified by local, cone-induced stress fields. The dykes have a minimum thickness of 5 cm and a maximum of 8 m and anastomose to form thicker, multiple intrusions (Fig. 5b, c, e). Plugs are connected to each other by straight to strongly curved, vertically jointed intrusions that are on average 1–3 m thick and change between discontinuous (dyke) to continuous (sill) intrusions along their propagation pathways (Fig. 5a, d). An up to 5-m-thick, NNE–SSW striking dyke can be followed throughout the outcrop area and may mark one of the major magma pathways that connected and fed the cone conduits (Fig. 5a). Multiple injection pulses flaring in the upper 20 m below the paleo-surface (Table 1) are common. The dykes have sharp contacts with the surrounding scoria and spatter deposits and often show chilled, multiple margins of 2–10 cm thickness. With contact to scoria, they often develop a "fingering" pattern. This is especially common with dyke splays (up to 0.5 m long dyke and sill protrusions) within the scoria cones (Fig. 5e). The outer dyke margins are covered with hyaloclastite breccias and scoria remnants (Fig. 5).

Elongated, ellipsoidal vesicles in the central to topmost parts of the dykes and sills are frequently observed (Fig. 10).

Fig. 7 Pyroclastic deposits of the Rauðhólar volcanic chain. **a** Welded agglutinated scoria and bombs used to infer the proximity of eruptive vent structures. **b** Welded lapilli exposed at resistant cone walls. **c** Possible clastogenic lava flow resting on top of a scoria breccia layer, which included clasts derived from river gravel. View to the NE
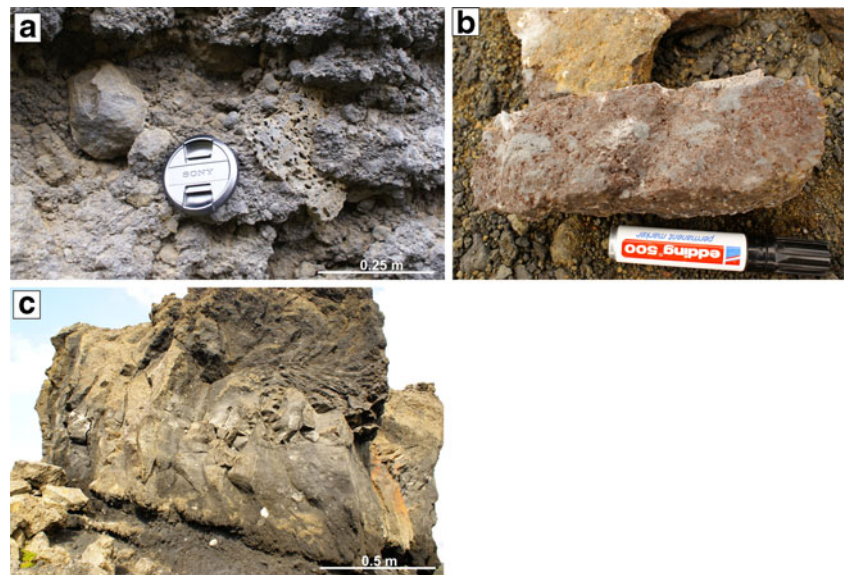

A few dykes emplaced in the pyroclastic portions of the cones display features such as breccias and tension gashes (Fig. 10), which suggest near-surface, horizontal magma flow towards the individual conduits. Shear deformation during flow caused preferred orientation of platy crystals and flattening and elongation of gas bubbles parallel to the shearing surface. The interaction of infiltrating rainwater with the still-hot scoria resulted in the formation of hydrothermal breccias and an often documented "white seam" around the volcaniclastic breccias, which is frequently seen along eroded cones and dykes (e.g., Guilbaud et al. 2009).

Multi-tiered lava flows in the southernmost volcanic chain

The most common morphology observed for Rauðhólar plug lavas along the cone row is a multi-tiered structure with a clear distinction between colonnade and hackly fractured entablature (Figs. 11 and 12), which is inferred to result from convective cooling by water interaction (e.g., Saemundsson 1970; DeGaff and Aydin 1987; Lescinsky and Fink 2000; Lyle 2000; Spörli and Rowland 2006). The plugs of the volcanic row can be divided into flow base (broad columns and flow bands), interior (massive, well-crystallized matrix and platy joints), side (glassy margin of columnar joints), and top (mainly breccias; Lescinsky and Fink 2000; Lyle 2000). Their margins consist of conical to irregularly shaped lava lobes with well-developed columnar joints that grade into intensely fractured obsidian and hyaloclastite breccias near the easterly outcrops that face the river. This architecture and the local occurrence of hyaloclastite are the result of rapid cooling and high heat flux by water–magma interaction (e.g., Lyle 2000; Gudmundsson 2003; Oskarsson 2009).

Fig. 8 Pyroclastic deposits of the Rauðhólar volcanic chain. **a** Cored bomb—inner core is clast derived from river gravel. **b** Elongated fluidal bomb. **c** Accidental block derived from the underlying tholeiitic lava flow embedded in scoria. **d** Rounded clasts derived from gravel deposits associated with the paleo-channel of the Jökulsá á Fjöllum River. These clasts were ballistically transported during a "wet" eruption
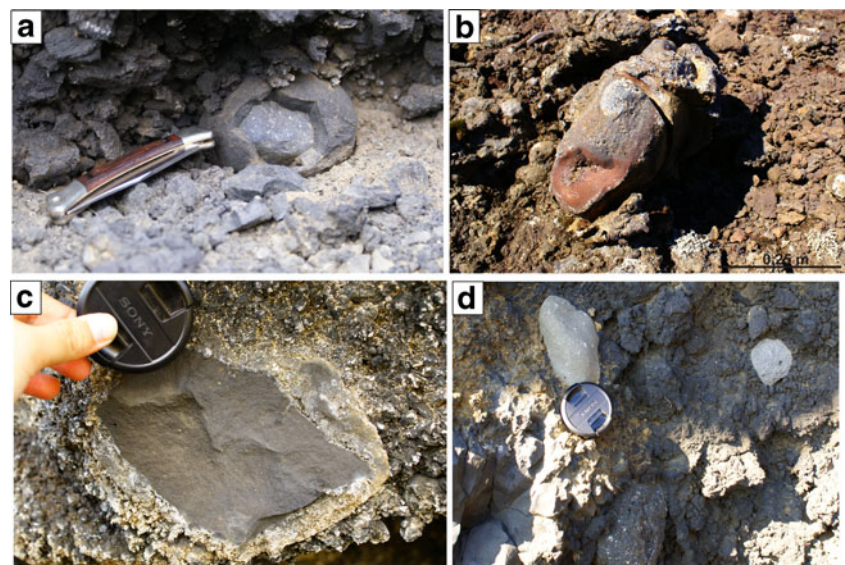
Fig. 9 Granular flow deposits. **a** Planar beds gently dipping to the west (for the location. see Fig. 6a). **b** Well-rounded lapilli appear as trails on top of swell structures. **c** Ripple cross-stratification as seen from the top

Reconstruction of the eruption style

The scattered exposures of pyroclastic deposits and the effects of differential erosion of the system only allow a simple eruption history to be reconstructed. Idealized composite cross-sections are presented in Fig. 12 to illustrate the inferred chronology of the eruption. It should be pointed out that whether the entire fissure was active contemporaneously or not, or where the eruption actually began cannot be inferred definitely from the field data. However, there are some indications for the progress of the eruption.

The overall irregular and horseshoe-shaped plug outlines in map view, as documented in portion of the Hljóðaklettar volcanic chain (Figs. 2b and 3 and the Supplementary data), are characteristic of early formed cones and lava effusions that issue from the same vent (Pioli et al. 2009). Rounded to angular accidental fragments and some of the cored bombs were derived from the underlying river bed and tholeiitic lava flows. These are restricted to the lower cone exposures in the central part of the study area (Fig. 2b, marked with a star). The occurrence of poorly sorted deposits containing abundant lithic clasts (Fig. 8c, d) indicates the onset of the eruption (Fig. 2b; Table 2) in this part of the Rauðhólar
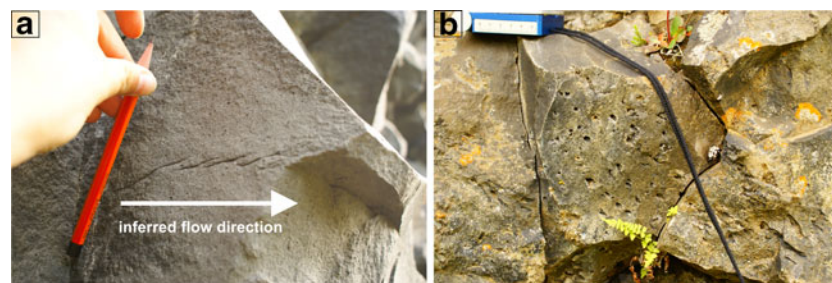
Fig. 10 Magma flow indicators documented in dykes. **a** En echelon, sigmoidal-shaped cracks. Pencil for scale. **b** Elongated, elliptical vesicles trace the magma flow path. Compass for scale

Fig. 11 a Distinction between colonnade and entablature joint systems; the lava wall is around 15 m high. b Chaotic curvi-columnar joints of the entablature dominate the shape of the approximately 10-m-wide necks. c Close-up view of the 3-m-high colonnade and entablature arrays

volcanic chain, where the feeder dyke intruded near the river.

After this initial phreatomagmatic eruption, pathways were cleared and scoria was ejected and accumulated. The effusive activity centralized to form a proper cone from which small lava flows emerged (Fig. 12; Table 2). Lava flows are characterized by colonnades and hackly fractured entablatures, they make up the interior of the Jökulsá canyon located in the southern part of the eroded cone row. These areas represent the immediate contact among erupted lava surface of magma with surficial water at the paleo-river bed. Lava flows most likely ponded in topographic depressions (Walker 1993), causing the thick colonnade and entablature features. As more vents opened up along the fissure, the eruption mechanism changed from short-lived phreatomagmatic activity to a transitional Strombolian/Hawaiian eruption (Valentine and Gregg 2008; Fig. 12; Table 2). The transitional Strombolian/Hawaiian style is inferred from the pyroclastic deposits composed of welded, fluidal to rounded, coarse-grained lapilli to bomb-sized fragments (Figs. 6, 7a, b, and 12; Table 2).
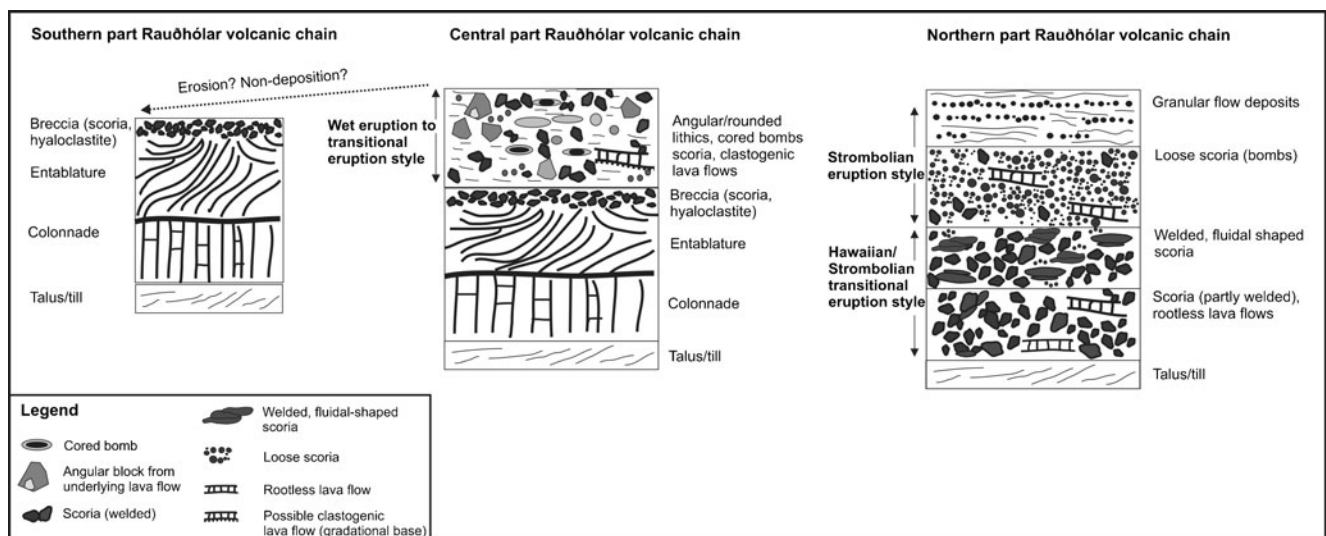
Fig. 12 Idealized composite section for the southern, central, and northern portions of the crater row used to illustrate the variation of eruptive styles through time

Fig. 13 Eroded scoria cone in the Sveinar cone row, southwest of Rauðhólar cone row. Dyke widens near the surface and feeds a spatter cone. View is towards the north, across the Jökulsárgljúfur canyon

Welded ramparts, often associated with "fire fountain" Hawaiian eruptions (Walker 1993), are found exposed along the central part of the Rauðhólar scoria cone row (Figs. 6d, e and 7a, b).

A final Strombolian phase deposited loose scoria deposits (Fig. 12; Table 2), which are only preserved in the Rauðhólar cones at the northern end of the volcanic chain. Scoria fall deposits accumulated mainly within 100–500 m of the vents. Rootless lava flows interbedded with scoria fall deposits only occur in well-preserved cone complexes at the northern end of the Rauðhólar row (Fig. 6b, c), and possible clastogenic flows are documented only in the central part (Fig. 7c).

The northernmost cone area has small-scale remnants of cross-bedded deposits that are interpreted as granular flow on cone slopes (Figs. 9 and 12; Table 2). These were possibly deposited as pyroclastic surges during the late phase of the volcanic activity of the vents (e.g., Valentine et al. 2005). The majority of these well-sorted deposits were probably eroded. There is no evidence of other granular flow deposition further to the south along the Jökulsá canyon or in areas adjacent to the Rauðhólar volcanic chain. Therefore, a local source near the northern part of the scoria cone row is inferred.

The dense plug network preserves shallow magma pathways that produced scoria cones analogous to the well-preserved Rauðhólar scoria cones (Figs. 4a and 5). In the southern part of the volcanic chain and along the river-facing front, small (2–5 m diameter; Table 1), plug-like bodies of basalt (breccia) occur that have formed as proximal vents or lava breakout (Fig. 5c). Magma pathways can be traced by a large number of cross-cutting, segmented, wavy to planar dyke and sill networks in the central eroded part of the volcanic chain (Fig. 5a, e). Multiple chilled margins in one dyke record incremental magma injection

pulses and document a complex feeding system. Whereas the overall dyke trend appears to be orthogonal, a subordinate radial dyke and sill pattern is restricted to the inner scoria cone plumbing system (Fig. 2b). The latter is attributed to the near-field stresses of the topographic load of the cones and magma overpressures (e.g., Acocella and Tibaldi 2005; Hintz and Valentine, 2012). Long (up to 1.5 km), tabular dykes with constant widths of up to 8 m are inferred to be regional "connecting feeders" between conduit complexes.

The linearly aligned eroded plugs in the Hljóðaklettar area trace the fissure eruption segments. The eruptive centers typically narrow on one side and extend into elongated, narrower fissure vents characterized by dense basalt dykes. Widening (flaring) of dykes to conduits within the uppermost 50 m (below paleo-surface) has been documented in several examples of (partly) eroded volcanic edifices (e.g., Keating et al. 2008; Geshi et al. 2010; Hintz and Valentine 2012) and fits well with our dataset, which show flaring between 5 and 20 m below paleo-surface. An analogue vertical cross-section through the uppermost 100 m of a well-preserved spatter cone and its feeder dyke can be observed at the 6,000- to 8,000-year-old (e.g. Sigurdsson et al. 1975) Sveinar–Randarhólar volcanic chain, also located along the Jökulsá canyon, just south of the Rauðhólar cone row studied here (Gudmundsson et al. 2008; Fig. 13). At Sveinar–Randarhólar, the dyke widens from 4 to 5 m near the river at 100 m depth to 13 m at the transition with the spatter cone near the surface, at a vertical distance of about 25–30 m (Gudmundsson et al. 2008; Fig. 13), which follows the observations in the Rauðhólar volcanic chain.

Factors that controlled the eruptive location

The Rauðhólar volcanic chain is situated on the western periphery of the Fremrinámur rift system in the Northern Volcanic Zone. The arcuate shape of the eruptive fissure is unusual in this area, which is otherwise dominated by linear volcanic and structural features (cone rows, eruptive fissures, grabens, and normal faults; Figs. 1, 2, and 3). The northernmost Rauðhólar cone complex and the en echelon-arranged necks in central Hljóðaklettar roughly follow the main north–south trend of the normal faults and graben systems of the fissure swarms in the Fremrinámur rift zone. Plugs and necks at the southern end of the eroded Hljóðaklettar cone row, however, coincide with the river channel of the Jökulsá canyon (Figs. 1b and 2b), which forms an angle (approximately NW–SE strike) to the main rift tectonic grain.

The area around the Rauðhólar and the Sveinar–Randarhólar volcanic chains are characterized by a general decrease in faulting (Figs. 1b and 2b), as magma emplacement

accommodated most of the tectonic strain on the western periphery of the fissure swarm. The observed normal faulting is concentrated in areas just west of the Rauðhólar volcanic chain, which is related to younger rifting events (e.g., Krafla rifting event 1975–1984), because they cut through interglacial lavas. The greater area of the Fremrinámur volcanic system comprises two adjacent extensional fissure focal points, one further to the south of the Rauðhólar cone row (Fig. 1b, dotted red line) and a second on the easternmost edge of the volcanic system, next to the hyaloclastite mountain of Dalfjall (Fig. 1b, red "R" and dotted line). These heavily faulted rift arms (grabens, relay ramps) that strike approximately N–S and, therefore, were extended along an E–W vector, are linked by an accommodation zone at the location of the Sveinar–Randarhólar eruptive fissure. At this location, the overall N–S trend of all the volcanic and structural features shifts to a prominent NNE–SSW strike and faults tend to step outside the fault-bounded narrow graben (Fig. 1b). In the eastern area of the Fremrinámur rift system, faults tend to run oblique to the main N–S rift strike, similar to parts of the Rauðhólar eruptive fissure. In summary, the Rauðhólar scoria cones follow the trace of a left-stepping (to the south) and right-stepping (to the north) extensional relay pattern. We postulate that changes in differential stresses along the strike of this fault system during overall extension was one of the major controls for the formation of the magma pathway and created the observed en echelon pattern of the craters of Rauðhólar.

The utilization of preexisting faults as magma conduits through the shallow crust to the surface is another possible explanation for variations in eruptive fissure geometry (e.g., Mastin and Pollard 1988; Valentine and Krogh 2006; Gaffney et al. 2007). Korme et al. (2004) suggests that the presence of "open structures" such as fault intersections, releasing bends, or extensional relays present conduits for magma ascent to form aligned volcanic chains. Differential extension in Northern Iceland involves several adjoining fissure swarms (two-armed Fremrinámur, Krafla to the west and Askja to the east) in the confined active northern rift zone, which causes local stress concentrations between the extensional blocks and hence rotation of the principal stresses. Similar en echelon volcanic chains on a large style are known from the Laki 1783 and Eldgjá 934 fissure eruptions that owe their origin to kinematics oblique to the rift zone (e.g., Thordarson and Self 1993; Jónasson et al. 1997).

Observed changes in the trends of eruptive fissures in SW Iceland and in the Krafla fissure swarm are related to the combined influence of preexisting geological features, stress field perturbations within volcanic edifices and other topographic features, and variation in crustal thickness (e.g., Jenness and Clifton 2009; Rooney et al. 2011). Valentine and Keating (2007) and Keating et al. (2008) describe similar observations within eroded monogenetic cones

located in intracontinental volcanic fields. Changes in cone alignment strike that is related to topographic barriers and to the possible structural influence of topography have been observed in several volcanic areas, such as Madeira (Klügel et al. 2005) and Hawaii (Walter and Amelung 2007). This effect has been modeled by Pinel and Jaupart (2004) and Gaffney and Damjanac (2006). It follows that the preexisting Jökulsá paleo-canyon could also have had an impact on the change of strike along the southern portion of the Rauðhólar volcanic chain.

Conclusions

The northern and central part of the Rauðhólar volcanic chain follows the major tectonic NNE trend of the Fremrinámur fissure system in the Northern Volcanic rift zone (Fig. 1b). The southernmost eroded part (Hljóðaklettar) coincides with the trend of the Jökulsá river and has an arcuate shape that trends NW–SE. The Rauðhólar volcanic chain can be subdivided into three sections that reflect decreasing depth of erosion-induced exposure from south to north (Figs. 4 and 12): (1) the southernmost Hljóðaklettar area contains only vents and plugs with a thin pyroclastic cover and multi-tiered lava flows; (2) the central part is formed by bombs and river gravel deposits in the lower cone sections that transitions northwards to welded to loose and flattened scoria (lapilli) neighboring the well-preserved scoria cones, small clastogenic lava flows, and an intersecting dyke–sill network (up to 8 m thick); and (3) at the northernmost end of Rauðhólar, well-preserved, coalescing scoria cones, up to 200 m high, composed of thick deposits of loose to weakly welded and flattened lapilli, with interbedded small rootless lava flows; a minor occurrence of reworked granular flow deposits is found along the river margin.

The distribution and nature of the volcanic features suggest that the cone row probably developed from a fissural eruption with short-lived initial phreatomagmatic phases that was restricted to the central part of the eruptive fissure, where the chain intersects the river system. This conclusion is based on the high amount of lithic clasts and accidental rounded clasts derived from the river bed and underlying tholeiitic lava flows. As more vents opened up, the eruption localized and shifted towards a transitional Hawaiian/Strombolian style and deposited welded scoria, fluidal bombs and spatter, and small clastogenic flows.

The arcuate shape of the Rauðhólar scoria cone row is probably the result of local stress changes between major grabens/relay zones that focused the eruption towards the western periphery of the fissure swarm. As the northern rift zone is affected by slightly oblique extension and there are three different volcanic systems interacting with each other

in this area, local stress conditions caused the rotation of the principal stress and formed faults and eruptive fissures that are slightly oblique to the main N–S rift trend, as seen in the eastern relay ramp area. The two adjacent, heavily faulted rift arms of the Fremrinámur fissure were linked by a relay zone that was exploited by the eruptive Rauðhólar and Sveinar–Randarhólar volcanic chains. Thus magma emplacement accommodated part of the tectonic strain.

References

Acocella V, Tibaldi A (2005) Dike propagation driven by volcano collapse: a general model tested at Stromboli, Italy. Geophys Res Lett 32:L08308. doi:10.1029/2004GL022248

Alho P, Russell AJ, Carrivick JL, Käyhkö J (2005) Reconstruction of the largest Holocene jökulhlaup within Jökulsa a Fjöllum, NE Iceland. Quat Sci Rev 24:2319–2334

Arnadottir T, Lund B, Jiang W, Geirsson H, Björnsson H, Einarsson P, Sigurdsson T (2009) Glacial rebound and plate spreading: results from the first countrywide GPS observations in Iceland. Geophys J Int 177:691–716

Björnsson A, Saemundsson K, Einarsson P, Tryggvason E, Gronvald K (1977) Current rifting episode in North Iceland. Nature 266:318–323

Bosworth W, Burke K, Strecker M (2003) Effects of stress fields on magma chamber stability and the formation of collapse calderas. Tectonics 22:1042

Brandsdottir B, Mencke W, Einarsson P, White RS, Staples R (1997) Färoe-Iceland ridge experiment 2. Crustal structure of the Krafla central volcano. J Geophys Res 102(B4):7867–7886. doi:10.1029/96JB03799

Brenna M, Cronin SJ, Smith IEM, Sohn YK, Nemeth K (2010) Mechanisms driving polymagmatic activity at a monogenetic volcano, Udo, Jeju Island, South Korea. Contrib Mineral Petrol 160:931–950

Buck WR, Einarsson P, Brandsdottir B (2006) Tectonic stress and magma chamber size as controls on dyke propagation: constraints from the 1975–1984 Krafla rifting episode. J Geophys Res 111(B12). doi:10.1029/2005JB003879

Connor CB, Conway M (2000) Basaltic volcanic fields. In: Sigurdsson H, Houghton B, McNutt S, Rymer H, Stix J (eds) Encyclopedia of volcanoes. Academic, San Diego, pp 331–343

DeGaff JM, Aydin A (1987) Surface morphology of columnar joints and its significance to mechanism and direction of joint growth. Geol Soc Am Bull 99:605–617

DeMets C, Gordon R, Argus D, Stein S (1994) Effects of recent revisions to the geomagnetic reversal time scale on estimates of current plate motions. Geophys Res Lett 21:2191–2194

Erlund EJ, Cashman KV, Wallace PJ, Pioli L, Rosi M, Johnson E, Delgado Granados H (2010) Compositional evolution of magma from Parícutin Volcano, Mexico: the tephra record. J Volcanol Geoth Res 197:167–187

Fedotov SA, Markhinin Y (1983) Great Tolbachik Fissure Eruption: geological and geophysical data, 1975–1976. Cambridge University Press, Cambridge

Gaffney ES, Damjanac B (2006) Localization of volcanic activity: topographic effects on dyke propagation, eruption and conduit formation. Geophys Res Lett 33(14):L14313. doi:10.1029/2006GL026852

Gaffney ES, Damjanac B, Valentine GA (2007) Localization of volcanic activity: 2. Effects of pre-existing structure. Earth Planet Sci Lett 263:323–338

Geshi N, Kusumoto S, Gudmundsson A (2010) Geometric difference between non-feeder and feeder dykes. Geology 38:195–198

Gudmundsson M (2003) Melting of ice by magma–ice–water interactions during subglacial eruptions as an indicator of heat transfer in subaqueous eruptions. In: White JDL, Clague D (eds) Explosive subaqueous volcanism. AGU Geophysical Monograph 140:61–72

Gudmundsson A, Friese N, Galindo I, Philipp S (2008) Dike-induced reverse faulting in a graben. Geology 36:123–126

Guilbaud M-N, Siebe C, Agustin-Flores J (2009) Eruptive style of the young high-Mg basaltic-andesite Pelagatos scoria cone, southeast of Mexico City. Bull Volcanol 71:859–880

Head JW, Wilson L (1989) Basaltic pyroclastic eruptions: influence on gas-release patterns and volume fluxes on fountain structure, and the formations of cinder cones, spatter cones, rootless flows, lava ponds, and lava flows. J Volcanol Geotherm Res 37:261–271

Heidbach O, Tingay M, Barth M, Reinecker J, Kurfeß D, Müller B (2008) The 2008 release of the world stress map. Available at http://www.world-stress-map.org

Hintz AR, Valentine GA (2012) Complex plumbing of monogenetic scoria cones: new insights from Lunar Crater Volcanic Field (Nevada, USA). J Volcanol Geotherm Res 239–240:19–32

Hjartardottir AR (2008) The fissure swarm of the Askja central volcano. M.Sc. thesis, University of Iceland, Reykjavik, Iceland

Höskuldsson T, Thordarson A (2002) Classic geology in Europe 3. Terra, Harpenden

Houghton BF, Wilson CJN, Smith IEM (1999) Shallow seated controls of explosive basaltic volcanism: a case study from New Zealand. J Volcanol Geotherm Res 91:97–120

Jenness MH, Clifton AE (2009) Controls on the geometry of a Holocene crater row: a field study from southwest Iceland. Bull Volcanol 71:715–728

Johannesson H, Saemundsson K (1998) Geological map of Iceland, 1:500,000. Tectonics. Institute of Natural History, Reykjavik

Johnson ER, Wallace PJ, Cashman KV, Delgado Granados H, Kent AJR (2008) Magmatic volatile contents and degassing-induced crystallization at Volcán Jorullo, Mexico: implications for melt evolution and the plumbing systems of monogenetic volcanoes. Earth Planet Sci Lett 269:478–487

Jónasson S, Einarsson P, Sigmundsson F (1997) Extension across a divergent plate boundary, the Eastern Volcanic Rift Zone, South Iceland, 1967–1994, observed with GPS and electronic distance measurement. J Geophys Res 102(B6):11913–11929

Keating GN, Valentine GA, Krier DJ, Perry FV (2008) Shallow plumbing systems for small-volume basaltic volcanoes. Bull Volcanol 70:563–582

Kirkbride MP, Dugmore AJ, Brazier V (2006) Radiocarbon dating of mid-Holocene megaflood deposits in the Jökulsa a Fjöllum, north Iceland. Holocene 16:605–609

Klügel A, Walter TR, Schwarz S, Geldmacher J (2005) Gravitational spreading causes en-echelon diking along a rift zone of Madeira Archipelago: an experimental approach and implications for magma transport. Bull Volcanol 68:37–46

Korme T, Acocella V, Abebe B (2004) The role of pre-existing structures in the origin, propagation and architecture of faults in the main Ethiopian rift. Gondwana Res 7:467–479

Lescinsky DT, Fink JH (2000) Lava and ice interaction at stratovolcanoes: use of characteristic features to determine past glacial extents and future volcanic hazards. J Geophys Res 105(B10):23711–23726. doi:10.1029/2000JB900214

Luhr JF, Simkin T (1993) Paricutin, the volcano born in a Mexican cornfield. Geoscience, Phoenix

Lyle P (2000) The eruption environment of multi-tiered columnar basalt lava flows. J Geol Soc Lond 157:715–722

MacLennan J, Jull M, McKenzie D, Slater L, Grönvold K (2002) The link between volcanism and deglaciation in Iceland. Geochem Geophys Geosyst 3(11):1–25. doi:10.1029/2001GC000282

Martin U, Nemeth K (2006) How Strombolian is a "Strombolian" scoria cone? Some irregularities in scoria cone architecture from the Transmexican Volcanic Belt, near Volcán Ceboruco, (Mexico) and Al Haruj (Libya). J Volcanol Geotherm Res 155:104–118

Mastin LG, Pollard DD (1988) Surface deformation and shallow dyke intrusion processes and Inyo Craters, Long Valley, California. J Geophys Res 93:13221–13235

Mazzarini F (2007) Vent distribution and crustal thickness in stretched continental crust: the case of the Afar Depression. Geosphere 3(3):152–162

Nakamura K (1977) Volcanoes as possible indicators of tectonic stress orientation—principle and proposal. J Volcanol Geotherm Res 2:1–16

Nemeth K, White JDL (2003) Geochemical evolution, vent structures, and erosion history of small-volume volcanoes in the Miocene Intracontinental Waipiata Volcanic Field, New Zealand. Geolines 15:98–101

Oskarsson BV (2009) The Skerin ridge on Eyjafjallajökull, south Iceland: morphology and magma–ice interaction in an ice-confined silicic fissure eruption. M.Sc. thesis, University of Iceland, Reykjavik

Paulsen TS, Wilson TJ (2010) New criteria for systematic mapping and reliability assessment of monogenetic volcanic vent alignments and elongate volcanic vents for crustal stress analysis. Tectonophysics. doi:10.1016/j.tecto.2009.08.025

Pinel V, Jaupart C (2004) Magma storage and horizontal dyke injection beneath a volcanic edifice. Earth Planet Sci Lett 221(1–4):245–262

Pioli L, Erlund E, Johnson E, Cashman K, Wallace P, Rosi M, Delgado Granados H (2008) Explosive dynamics of violent Strombolian eruptions: the eruption of Paricutin Volcano 1943–1952 (Mexico). Earth Planet Sci Lett 271(1–4):359–368

Pioli L, Azzopardi BJ, Cashman KV (2009) Controls on the explosivity of scoria cone eruptions: magma segregation at conduit junctions. J Volcanol Geotherm Res 186:407–415

Rooney TO, Bastow ID, Keir D (2011) Insights into extensional processes during magma assisted rifting: evidence from aligned scoria cones. J Volcanol Geotherm Res 201:83–96

Saemundsson K (1970) Interglacial lava flows in the lowlands of southern Iceland and the problem of two-tiered columnar jointing. Jökull 20:62–77

Saemundsson K (1979) Outline of the geology of Iceland. Jökull 29:7–28

Self S, Sparks RSJ, Booth B, Walker GPL (1974) The 1973 Heimaey Strombolian scoria deposits, Iceland. Geol Mag 111:539–548

Sigurdsson O, Zophoniasson S, Hannesdottir L, Thorgrimsson S (1975) Geological report on the proposed hydroelectric power plant at Dettifoss. Report OS-ROD-7526. National Energy Authority (Orkustofnun), Reykjavik (in Icelandic)

Slater L, Jull M, McKenzie D, Grönvold K (1998) Deglaciation effects on mantle melting under Iceland: results from the northern volcanic zone. Earth Planet Sci Lett 164:151–164

Spörli K, Rowland J (2006) "Column on column" structures as indicators of lava/ice interaction, Ruapehu andesite volcano, New Zealand. J Volcanol Geotherm Res 157:294–310

Tentler T, Mazzoli S (2005) Architecture of normal faults in the rift zone of central north Iceland. J Struct Geol 27:1721–1739

Thorarinsson S (1951) Laxárgljúfur and Laxarhraun—a tephrochronological study. Geogr Ann A 1–1:1–89

Thorarinsson S (1959) Some geological problems involved in the hydroelectric development of the Jökulsa a Fjöllum, Iceland. Report to the State Electricity Authority, Reykjavik, Iceland

Thorarinsson S (1971) Aldur ljósu gjóskulaganna úr Heklu samkvæmt leiðréttu geislakolstímatali. Náttúrufræðingurinn 41:99–105 (in Icelandic)

Thordarson T, Larsen G (2007) Volcanism in Iceland in historical time: volcano types, eruption styles and eruptive history. J Geodyn 43:118–152

Thordarson T, Self S (1993) The Laki (Skaftar Fires) and Grimsvötn eruptions in 1783–1785. Bull Volcanol 55:233–263

Tryggvason E (1980) Subsidence events in the Krafla area, North Iceland, 1975–1979. J Geophys 47:141–153

Tryggvason E (1994) Surface deformation at the Krafla volcano, North Iceland, 1982–1992. Bull Volcanol 56(2):98–107

Valentine GA, Gregg TKP (2008) Continental basaltic volcanoes—processes and problems. J Volcanol Geotherm Res 177:857–873. doi:10.1016/j.jvolgeores.2008.01.050

Valentine GA, Keating GN (2007) Eruptive styles and inferences about plumbing systems at Hidden Cone and Little Black Peak scoria cone volcanoes (Nevada, USA). Bull Volcanol 70:105–113. doi:10.1007/s00445-007-0123-8

Valentine GA, Krogh KEC (2006) Emplacement of shallow dykes and sills beneath a small basaltic volcanic center—the role of pre-existing structure (Paiute Ridge, southern Nevada, USA). Earth Planet Sci Lett 246:217–230. doi:10.1016/j.epsl.2006.04.031

Valentine GA, Krier D, Perry FV, Heiken G (2005) Scoria cone construction mechanisms, Lathrop Wells volcano. Geology 33:629–632. doi:10.1130/G21459.1

Vespermann D, Schmincke HU (2000) Scoria cones and tuff rings. In: Sigurdsson H, Houghton BF, McNutt SR, Rymer H, Stix J (eds) Encyclopaedia of volcanoes. Academic, San Diego, pp 683–694

Waitt RB (2002) Great Holocene floods along Jökulsa a Fjöllum, north Iceland. In: Martini IP, Baker VR, Garzón G (eds) Flood and megaflood processes and deposits: recent and ancient examples. Spec Pub Int Assoc Sediment 32:37–51

Walker GPL (1993) Basaltic-volcano systems. Geol Soc London Spec Pub 76:3–38

Walter TR, Amelung F (2007) Volcanic eruptions following M ≥9 megathrust earthquakes: implications for the Sumatra–Andaman volcanoes. Geology 35:539–542